ELSEVIER

Nuclear Physics A 581 (1995) 93-106

NUCLEAR PHYSICS A

Differential cross section and analyzing power for elastic scattering of protons on ^{6}Li below 2.2 MeV ⋆

M. Skill [a,1], R. Baumann [a], G. Keil [a], N. Kniest [a,2], E. Pfaff [a,3], M. Preiss [a], G. Reiter [a,4], G. Clausnitzer [a], M. Haller [b], W. Kretschmer [b]

[a] *Institut für Kernphysik, Strahlenzentrum der Universität Giessen, D-35392 Giessen, Germany*

[b] *Tandemlabor der Universität Erlangen-Nürnberg, D-91056 Erlangen, Germany*

Received 15 March 1994; revised 17 July 1994

Abstract

Differential cross section $d\sigma/d\Omega$ and analyzing power A_y of elastic ^{6}Li$(\vec{p},p)^6$Li scattering have been measured in the energy range 0.4 MeV$\leqslant E_p \leqslant$ 2.2 MeV. The angular distributions were obtained at thirteen different angles between $\theta_{lab} = 40°$ and 160° with statistical uncertainties of less than 2×10^{-3}. The data show a resonance-like behaviour in the excitation functions for $d\sigma/d\Omega$ and A_y near E_p = 1.8 MeV (i.e. $E_{c.m.}$ = 1.56 MeV). An energy-dependent phase-shift analysis has been performed from which resonance parameters have been deduced. The analysed data are well described in the whole energy range and support the predictions of recent refined resonating-group calculations.

Keywords: NUCLEAR REACTIONS ^{6}Li$(\vec{p},p)$; E_p = 0.4–2.2 MeV; measured analyzing power A_y, differential cross section $d\sigma/d\Omega$; deduced ^{7}Be resonance parameters Γ, Γ_p, J, π; enriched target.

1. Introduction

The knowledge of accurate cross section $d\sigma/d\Omega$ and analyzing power A_y of the elastic ^{6}Li$(\vec{p},p)^6$Li scattering is of basic interest for the understanding of the compound

⋆ Work supported by the Deutsche Forschungsgemeinschaft.

[1] Present address: Hermann Wels Strasse, 36358 Hermannstein, Germany.

[2] Present address: Bundesamt für Wirtschaft, Frankfurter Strasse 29-31, 65760 Eschborn, Germany.

[3] Present address: Pestalozzistrasse 4, 35640 Asslar, Germany.

[4] Present address: Cleeberger Strasse 19, 35647 Waldsolms Brdf., Germany.

SSDI 0375-9474(94)00422-6

nucleus ^{7}Be, especially for comparison with resonating-group calculations, e.g. carried out by Hoffmann et al. [1,2] and to remove ambiguities in the phase-shift analysis of the data in the energy region below 2.0 MeV [3]. Nuclear-fusion processes and the unsolved solar-neutrino problem provide additional interest for the structure of the $A = 7$ compound system. The reaction ^{6}Li(n,t)^{3}He is the dominant breeding process for tritium in fusion reactors and the capture reaction ^{3}He$(\alpha,\gamma)^7$Be is part of the pp-cycle and a key reaction for the understanding of the solar-neutrino problem.

Measurements of the differential cross section have been reported by Bashkin and Richards [4] (1.0–3.6 MeV), McCray [5] (0.45–2.9 MeV), Harrison and Whitehead [6] (2.4–12.0 MeV), Fasoli et al. [7] (1.3–5.6 MeV), Lerner and Marion [8] (1.36 MeV) and Haller et al. [3,9] (1.6–10 MeV). The earlier measurements were carried out in small angular ranges except those of Haller et al. [3,9], which have been performed for angles between 30° and 165° in energy steps of 100 keV with an adequate accuracy.

In the energy range in the vicinity of the predicted resonance at $E_x = 7.21$ MeV only two measurements of the analyzing power were carried out: Petitjean et al. [10] (1.2–3.2 MeV), Haller et al. [3,9] (1.6–10 MeV). As an extension of recent polarization measurements at higher energies [3,9] $\mathrm{d}\sigma/\mathrm{d}\Omega$ and A_y have been measured in the energy range 0.4 MeV$\leqslant E_p \leqslant$2.2 MeV at thirteen different angles ($40° \leqslant \theta_{lab} \leqslant 160°$) with an accuracy better than 2×10^{-3} typically. The data have been submitted to a phase-shift analysis including angular momenta $L \leqslant 2$. Various mixings, which may arise for the spin $\frac{1}{2} + 1$ case, have been considered additionally. The experimental data were presented in part in Refs. [11–13].

2. Experiment

2.1. Experimental arrangement

The measurement of the differential cross section and analyzing power for elastic ^{6}Li$(\vec{p},p)^6$Li scattering has been carried out at the Giessen polarization facility described in Refs. [14–16]. The polarized H^- current produced in the Lamb-shift ion source was typically 1 μA. After acceleration in the 1 MV tandem [17] the proton beam was analysed by a slit system and two 90° magnets. Up to 450 nA proton current was available in the scattering chamber after a small aperture. The average beam polarization was $P_y = 0.7$. The experimental setup in the scattering chamber is shown in Fig. 1. Angular distributions ($40° \leqslant \theta_{lab} \leqslant 160°$, in steps of 10°) of the analyzing power and the differential cross section were determined for energies between $E_p = 0.4$ and 2.2 MeV in steps of 100 keV.

The beam was focussed through two apertures of 2.5 and 3 mm diameter to the exchangeable target in the centre of the scattering chamber. Fourteen surface-barrier detectors [*Ortec, partially depleted* (100 μm, 100 mm^2)] surrounded the target with an overlap at $\theta_{lab} = 90°$ (left–right arrangement). Apertures limited the detector solid

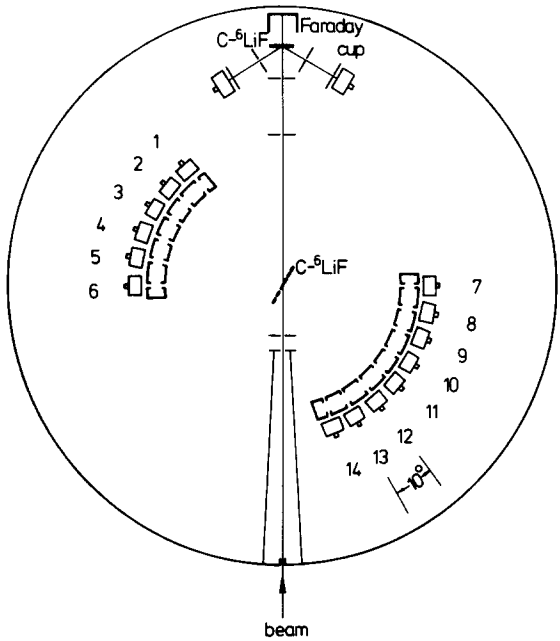

Fig. 1. Detector arrangement in the scattering chamber. The target is rotated by 60° with respect to the beam direction to enable the measurement of the angular distribution.

angles between 2×10^{-4} sr at 40° and 4×10^{-4} sr at 160° in order to adapt the counting rate to the speed of the detector electronics (3000 cps). The target was turned 60° relative to the beam axis; therefore the complete angular range could be measured simultaneously.

The polarization was measured "on-line" by the ^{6}Li($\vec{p}$,^{3}He)^{4}He reaction in a second arrangement behind the scattering target consisting of a ^{6}LiF target and two detectors at $\theta_{lab} = 120°$. The analyzing power of this reaction is well known [18]. The polarization was switched between "polarized" and "unpolarized" with a frequency of 62 Hz. The target current was integrated "on-line" with a Faraday cup.

2.2. *Target technology*

Solid targets of pure ^{6}Li are favourable for measurements of cross section and analyzing power of elastic ^{6}Li($\vec{p}$,p)^{6}Li scattering. However, it is very difficult to provide those targets because Li is hygroscopic and forms Li_2O in the air and LiOH with water from air moisture. Due to these chemical reactions pure ^{6}Li targets are very fragile and instable. Targets of the type C–^{6}Li–C, C–^{6}Li–paraffin and different thicknesses were tested to minimize the oxidation process. In spite of this provision pulse-height spectra of these targets showed peaks of protons elastically scattered off oxygen. The separation of this peak from the protons scattered elastically off ^{6}Li was not possible. Alternatively targets from the chemically stable ^{6}LiF were produced. These targets did not show the disadvantages mentioned above. The protons scattered off fluorine (A = 19,

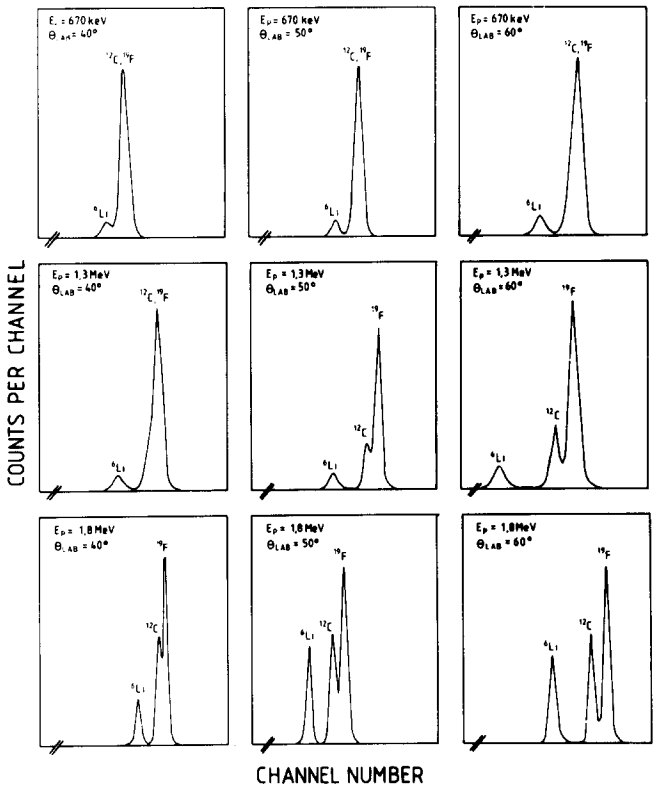

Fig. 2. Proton spectra scattered off a C–^{6}LiF target at different angles and energies.

Z=9) could be well separated from the protons scattered off lithium (A = 6, Z=3). In further investigations the ^{6}LiF targets were stabilized mechanically by using backings of carbon and aluminium (C–^{6}LiF–C, Al–^{6}LiF–Al, C–^{6}LiF) so that good separation of the ^{6}Li(p,p) peak was guaranteed. Using backings with higher atomic number Z increases the difference in energy between the protons scattered elastically off lithium and off the backing material. Tests showed that 70 nm aluminium (Z = 13) was necessary to completely cover of lithium. This produced a severe increase of the counting rate due to the Z^2 dependence of the Rutherford formula; therefore, an aluminium backing was not suitable. The C–^{6}LiF target with 10 nm carbon and 100 nm ^{6}LiF showed the best behaviour and clean spectra were obtained in the whole angular range. Typical examples are shown in Fig. 2.

2.3. *Analyzing-power measurements*

The analyzing power A_y was evaluated from the asymmetry ϵ of the one-detector arrangement described by

$$\epsilon = P_y \cdot A_y = \pm \left(\frac{I^\circ}{I^\uparrow} \cdot \frac{Z^\uparrow}{Z^\circ} - 1 \right), \tag{1}$$

where $I^\circ/I^\uparrow$ is the target current ratio, $Z^\uparrow/Z^\circ$ the counting rate ratio whereby $\uparrow$ and $\circ$ denotes the polarized and unpolarized cycle. The positive sign is taken for P_y parallel to the scattering normal defined by the Basel convention [19] (i.e. for scattering to the left). Using this "polarized–unpolarized method" the apparent asymmetries are less than 2×10^{-4} [14].

2.4. Cross-section measurements

Absolute cross-section measurements require a precise determination of the detector solid angles and the target thickness; furthermore an exact target current integration is necessary.

The differential cross section for the unpolarized beam is described by:

$$\left(\frac{\mathrm{d}\sigma}{\mathrm{d}\Omega} \right)^\circ = \frac{Z^\circ}{I^\circ N_A^\circ \Delta\Omega^\circ E^\circ}, \tag{2}$$

where Z° is the counting rate, I° the number of incident particles, N_A° the nuclei density (^{6}Li/cm^2, E° the efficiency and $\Delta\Omega^\circ$ the solid angle of one detector [20]. The target thickness and the efficiency were assumed to be constant during the experiment. The solid angles of the detectors were determined by elastic ^{79}Au(p,p)^{79}Au scattering at E_p = 0.9 MeV. The scattering cross section is well described by the Rutherford formula. In a calibration measurement all detectors were turned to the θ_{lab} = 90° position sequentially using the rotable bottom of the scattering chamber. The counting rates were normalized to the 40° detector. The target current was monitored by a fixed detector under θ_{lab} = 15°. The solid angle ratio is given by

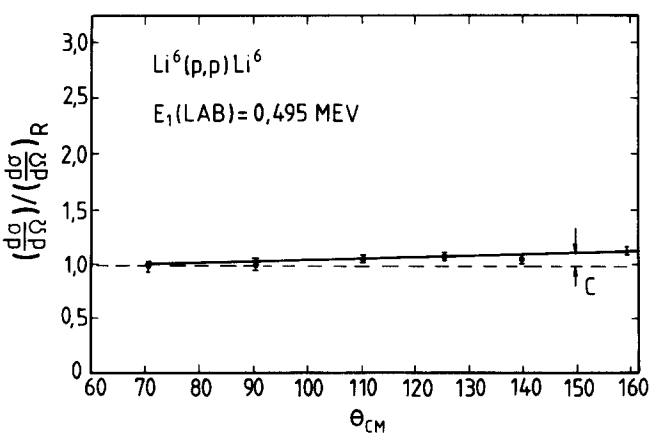

Fig. 3. $(\mathrm{d}\sigma/\mathrm{d}\Omega)/(\mathrm{d}\sigma/\mathrm{d}\Omega_R)$ as a function of $\theta_{c.m.}$ at E_p = 0.5 MeV.

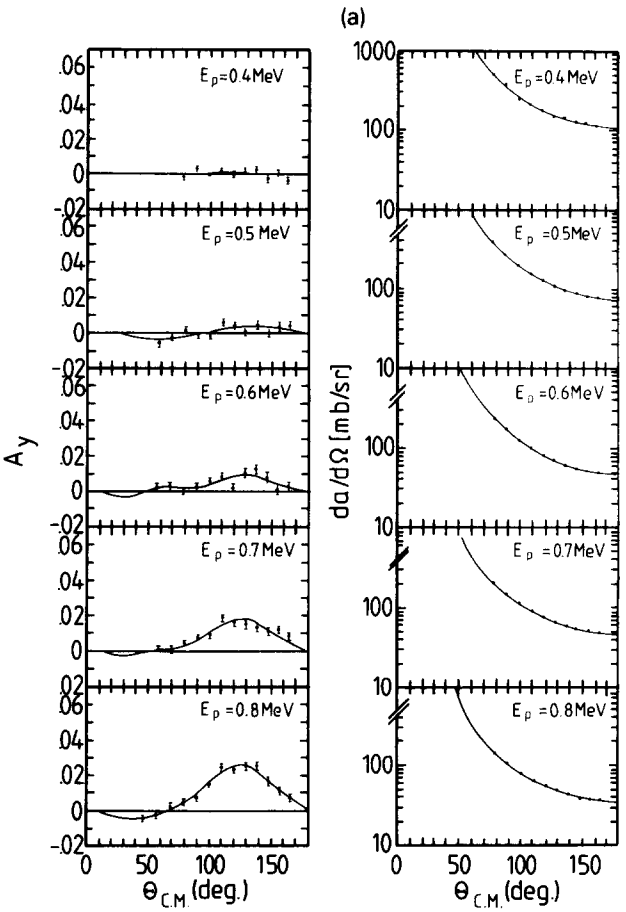

Fig. 4. Analyzing-power and cross-section data compared with the phase-shift analysis. The statistical errors are a factor 2 smaller than the symbols. All values are given in the centre-of-mass system.

$$\frac{\Delta\Omega_i}{\Delta\Omega_{40^\circ}} = \frac{Z_i \cdot Z^{15}_{40^\circ}}{Z_{40^\circ} \cdot Z^{15}} \tag{3}$$

with $\Delta\Omega_i$ the solid angle of the detector (i) actually rotated to $\theta_{lab} = 90°$, $\Delta\Omega_{40^\circ}$ is the solid angle of the 40° detector, Z_i is the counting rate of the detector (i) actually rotated to $\theta_{lab} = 90°$, Z_{40° is the counting rate of the 40° detector when in position 90°, Z^{15} is the counting rate of the 15° detector with detector (i) at 90° ($\propto$ target current), $Z^{15}_{40^\circ}$ is the counting rate of the 15° detector with the 40° detector at 90° ($\propto$ target current).

The accurate determination of the target thickness was not possible. The normalization of the absolute cross section was performed by adjusting the data to corresponding data of Ref. [5] by determination of a normalization factor at $\theta_{lab} = 40°$ and $E_p = 0.5$ MeV. With this factor the data could be normalized.

Furthermore the calibration factor was determined by a second method independent of target thickness and solid angle. Fig. 3 shows the ratio of the measured cross section of Ref. [5] ($d\sigma/d\Omega$) relative to the calculated Rutherford cross section ($d\sigma/d\Omega)_R$

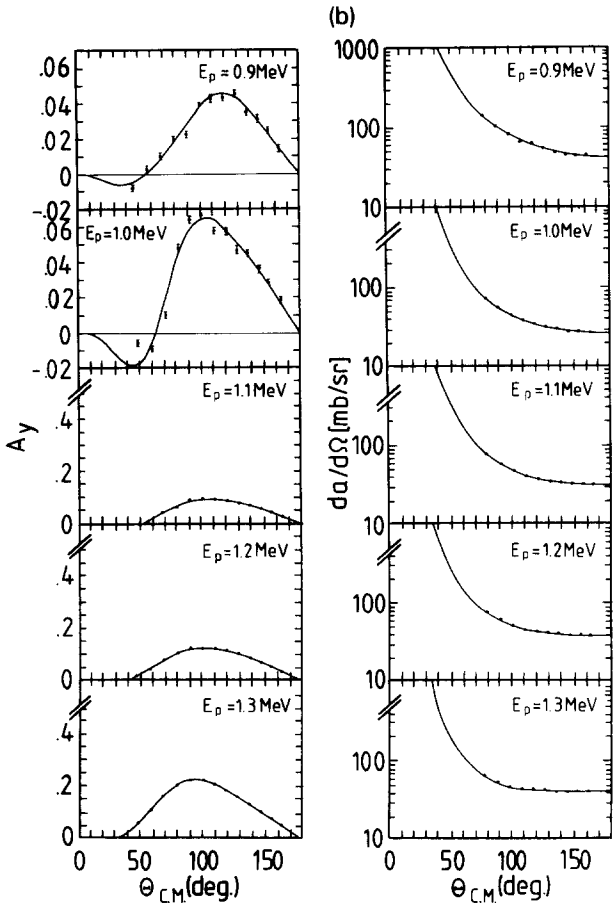

Fig. 4 — continued.

plotted as a function of $\theta_{c.m.}$ at E_p = 0.5 MeV. With this ratio the deviation C from the Rutherford cross section for all angles could be determined. Both methods agreed within an accuracy better than 5%.

2.5. *Corrections and errors*

The spectra of the elastic ^{6}Li(p,p)^{6}Li scattering were dead-time corrected and a linear background subtraction has been performed. The dead-time corrections (in the order of 1%) were calculated using the formulae and constants of the electronic equipment as described by Reiter [21].

The finite size of the solid angles have been taken into account for the angular distributions of A_y. Due to the small solid angles these corrections were less than 5×10^{-4}.

The final statistical errors of the observables were determined by quadratic addition of the statistical errors of the counting rate and the errors of all corrections. For the

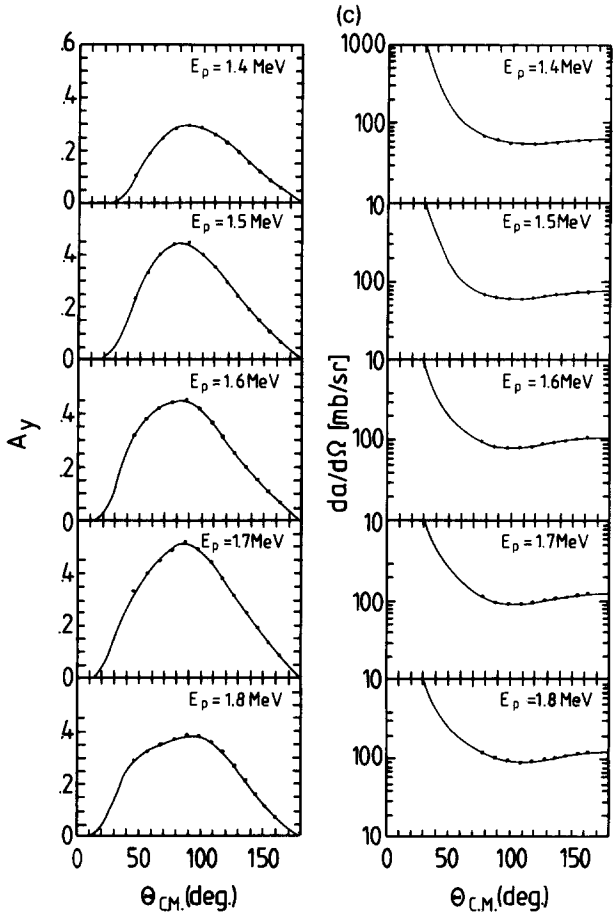

Fig. 4 — continued.

analyzing power statistical errors of $\Delta A_y \leqslant 1.5 \times 10^{-3}$ could be achieved, for the cross-section data the relative statistical errors are about 0.2%.

3. Experimental results

Differential cross section and analyzing power were measured at nineteen energies between 0.4 and 2.2 MeV in steps of 0.1 MeV. The angular range was $\theta_{lab} = 40°$ to 160° in steps of 10° ($d\sigma/d\Omega$: 70°–160°). The experimental values and their statistical errors are shown in Fig. 4. The data agree with the phase-shift analysis of an Erlangen group [3,9] (solid curve in Fig. 4).

A comparison of the A_y measurements with the data of Petitjean et al. [10] shows good agreement at E_p = 1.2, 1.6 and 1.8 MeV. At E_p = 1.4, 2.0 and 2.2 MeV small deviations at forward angles can be found. The cross-section measurements can be compared with the data of Haller [3,9] at 1.6, 1.8, 2.0 and 2.2 MeV. A shift in the

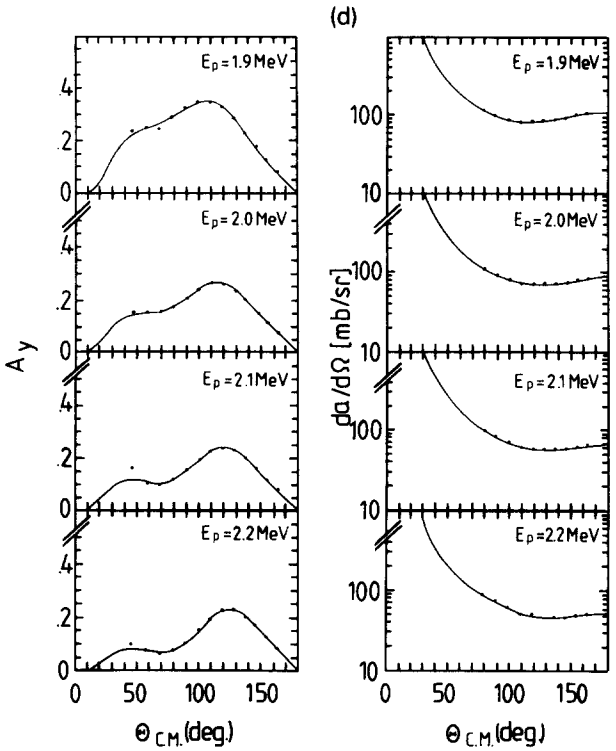

Fig. 4 — continued.

absolute values of both groups can be seen caused by the different calibration methods. The relative shape however is similar.

The excitation functions for A_y and $d\sigma/d\Omega$ show a resonance-peak at $E_{c.m.}$ = 1.56 MeV. This is most prominent in A_y at forward angles and occurs in $d\sigma/d\Omega$ only at backward angles (Fig. 5).

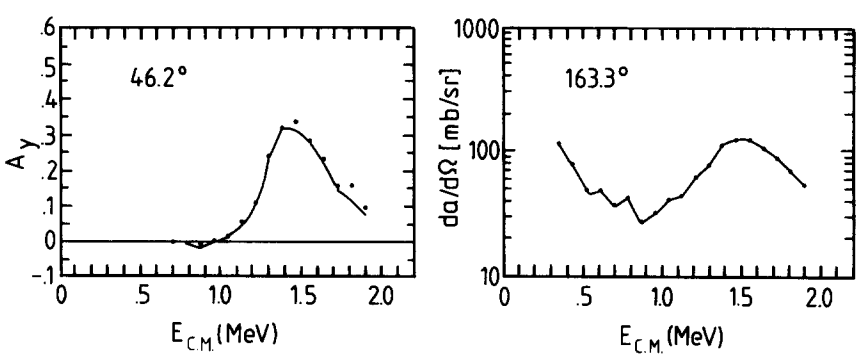

Fig. 5. Excitation function for A_y (46.2°) and $d\sigma/d\Omega$ (163.3°) compared with the phase-shift analysis. All values are given in the centre-of-mass system.

4. Phase-shift analysis

The spin-1 target nucleus ^{6}Li and the spin-$\frac{1}{2}$ protons can couple to channel spin $S = \frac{1}{2}$ (doublet) or $S = \frac{3}{2}$ (quartet). The coupling of the channel spin with the orbital angular momentum L results in the total angular momentum J. The states are denoted by $^{2S+1}L_j$. The possible configurations for $L = 0$, 1 and 2 are shown in Fig. 6.

While J and π are good quantum numbers mixing of states of different L and/or S is possible via tensor forces. The phase-shift analysis of the data including $L = 0$, 1, 2 and various mixings which may arise for this spin-$\frac{1}{2}$ +1 case has been performed with the computer code HALFONE (see Ref. [22]) developed at the ETH Zürich. In the energy range $0.4 \leqslant E_p \leqslant 2.8$ MeV (including the Erlangen measurements [3,9]) the data were fitted consecutively. The fitting algorithm minimizes the χ^2-type error function. Proceeding from one energy to the next the fitted values of the phase-shift parameters were taken as starting values for the subsequent energy. The resulting parameters are energy dependent, especially the $^4P_{5/2}$ phase shift shows a resonant behaviour. They were parametrized according the Breit–Wigner formula [23]

$$\exp(2i\delta(E)) = \exp(2i\lambda(E)) \left(\exp(-2\mu(E)) + \frac{i\Gamma_p}{E_R - E - \frac{1}{2}i\Gamma} \right). \tag{4}$$

In this formula the resonance is described by the total width Γ, the partial width Γ_p and the resonance energy E_R. The parameters were stable against a variation of the starting values in the fit procedure. The resonance parameters are given in Table 1. They are compared with an earlier investigation of this $\frac{5}{2}^-$ resonance which has been analysed by McCray [5] from cross-section measurements. His analysis was performed under the assumption that the state in ^{7}Be at 7.18 MeV is the mirror state of the $\frac{5}{2}^-$ state in ^{7}Li analysed by Johnson et al. [24]. A later investigation of scattering data in this energy region by Haller et al. [3,9], which included the analyzing-power data of Petitjean et al. [10], was consistent with the supposed $\frac{5}{2}^-$ value as well as the resonance parameters of McCray [5]. In contrast to the present work these previous investigations included none [5] or only few and unprecise [10] analyzing-power data. It turned out in the

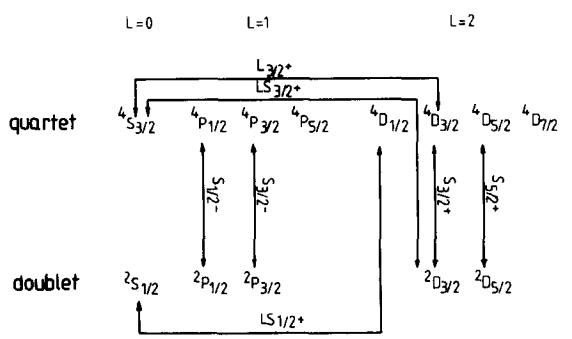

Fig. 6. Phase-shifts and mixing parameters of spin-$\frac{1}{2}$ on spin-1 scattering for S-, P- and D-waves.

Table 1
Resonance parameters for the dominant $E_{c.m.}$ = 1.56 MeV state

	This work	Analysis of $d\sigma/d\Omega$ data [5] (no errors quoted)	Resonating-group calculations [26]
E_R [MeV]	1.56 ± 0.1	1.57	1.39
Γ [MeV]	0.4 ± 0.05	0.84	0.51
Γ_p [MeV]	0.19 ± 0.05	0.8	0.46

analysis, however, that the determination of both, the resonance parameters and the J^π value, is ambiguous if only cross-section data are fitted. In the present investigation these ambiguities are resolved by the inclusion of high-precision analyzing-power and differential cross-section data in small angular steps. The deviation of the resulting Γ and Γ_p from the previously determined parameters (see Table 1) is probably due to the above-mentioned ambiguities in the analysis of the cross-section data [5] alone.

The errors of the resonance parameters given in Table 1 refer to a 10% increase of the χ^2 function, averaged over all energies (see also Ref. [3]). In the analysis orbital angular momenta up to $L = 2$ as well as the mixing parameters were taken into account although the contributions of the $L = 2$ phase shifts are not important in the energy range considered. The real part of the $^4P_{5/2}$ phase shift increases from 0° to 180° in the c.m. energy range from 1.3 to 1.8 MeV. The phase shifts are shown in Fig. 7.

A comparison with the predictions of refined resonating-group calculations [25] on the basis of a multi-structure and multi-channel approach (dashed line in Fig. 7) shows that the total width is overestimated and that the predicted resonance energy is about 200 keV too low. A detailed description of these calculations together with the restrictions necessary for the ^{7}Be system is given in the papers of Hofmann [1,2].

In Fig. 8 the resulting phase shift is represented in an Argand plot where the x- and

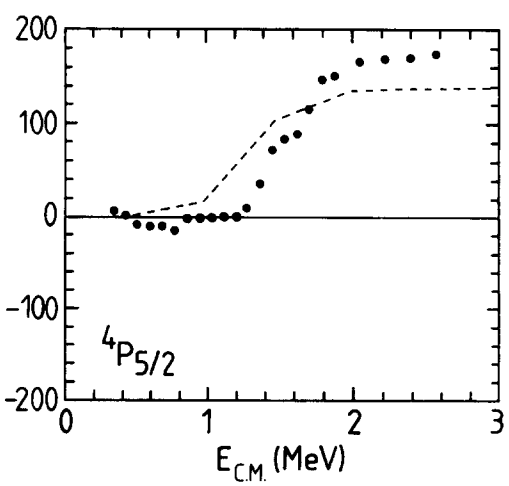

Fig. 7. Real part of the $^4P_{5/2}$ phase shift compared with theoretical predictions from Ref. [25].

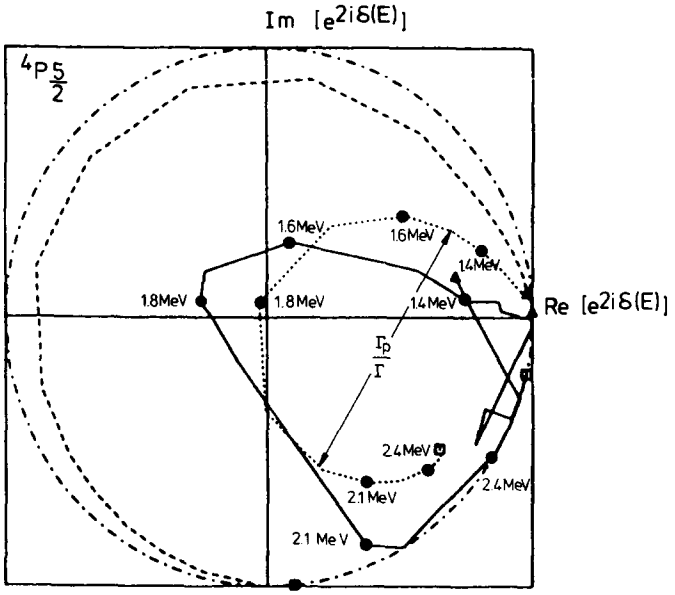

Fig. 8. Argand plot of the $^4P_{5/2}$ phase shift. The picture shows the single energy fit (solid curve) compared with a Breit–Wigner parametrization (dotted curve) and resonating-group predictions (dashed curve). $E_p = 0.4$ MeV (triangle), $E_p = 2.8$ MeV (square).

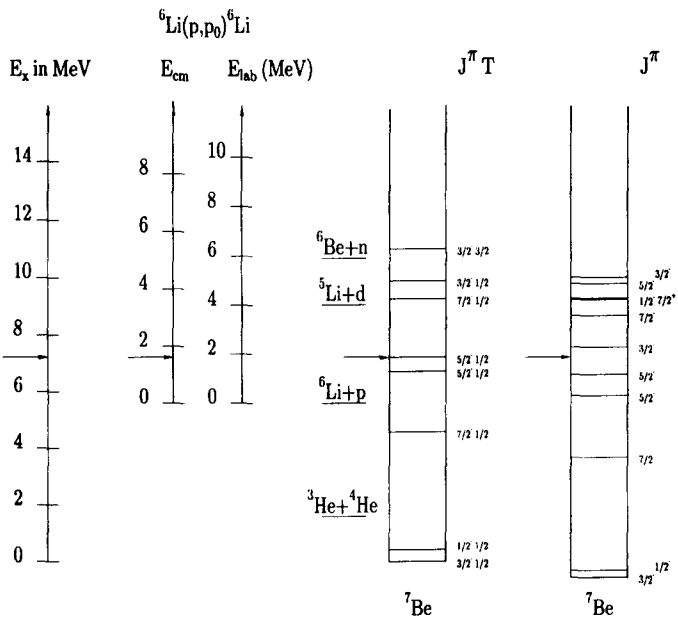

Fig. 9. Level scheme of ^{7}Be including the results of the present work compared with the predictions of the refined resonating-group model [1]. The obtained level is marked by an arrow.

y-axis denote the real and imaginary part of $\exp(2i\delta(E))$. Here $\delta(E)$ is the eigenphase shift as a function of c.m. energy. As shown in Fig. 8 real and imaginary parts of the resonant S-matrix exhibit a counterclockwise turn with increasing energy. The results obtained from the phase-shift analysis (solid curve) have been parametrized according to Breit–Wigner formula (dotted curve). Furthermore the theoretical predictions of Herrmann [26] (dashed curve) are represented.

5. Conclusions

Measurements of A_y and $d\sigma/d\Omega$ have confirmed the theoretically predicted resonance at $E_{c.m.} = 1.56$ MeV and the older investigations of this resonance by McCray [5] and Haller et al. [3,9]. In the frame of this work total angular momentum and the parity were fixed unambiguously. Resonance energy, total width and partial width of this resonance were established with good accuracy. Fig. 9 shows a comparison of the obtained resonance level in ^{7}Be with an experimental level scheme [27] and with the predictions of resonating-group calculations of Ref. [1].

The $J^\pi = {}^4P_{5/2}$ level is marked in the figure. The level at $E_x = 7.21$ MeV (i.e. $E_p = 1.8$ MeV, $E_{c.m.} = 1.56$ MeV) appears in the excitation functions of the cross section and the analyzing power. The phase-shift analysis is consistent with the assumed $J^\pi = \frac{5}{2}^-$.

Acknowledgements

We are indebted to U. Juritz for the preparation of the ^{6}LiF targets and to P. Keiner for his technical assistance.

References

[1] H.M. Hofmann, T. Mertelmeier and W. Zahn, Nucl. Phys. A 410 (1983) 208.
[2] H.M. Hofmann, Nucl. Phys. A 416 (1984) 363c.
[3] M. Haller, W. Kretschmer, A. Rauscher, R. Schmitt and W. Schuster, Nucl. Phys. A 496 (1989) 205.
[4] S. Bashkin and H.T. Richards, Phys. Rev. 84 (1951) 1124.
[5] J.A. McCray, Phys. Rev. 130 (1963) 2034.
[6] W.D. Harrison and B. Whitehead, Phys. Rev. 132 (1963) 2607.
[7] U. Fasoli, E.A. Silverstein, D. Toriolo and G. Zage, Nuovo Cim. 34 (1964) 1832.
[8] G.M. Lerner and J.P. Marion, Nucl. Instr. Meth. 69 (1969) 151.
[9] M. Haller, M. Betz, W. Kretschmer, A. Rauscher, R. Schmitt and W. Schuster, Nucl. Phys. A 496 (1989) 189.
[10] C. Petitjean, L. Brown and R.G. Seyler, Nucl. Phys. A 129 (1969) 209.
[11] M. Skill, R. Baumann, S. Hoos-Wenzel, G. Keil, N. Kniest, H. Lange, T. Ohly, E. Pfaff, M. Preiss, G. Reiter, G. Clausnitzer, M. Haller and W. Kretschmer, Proc. Int. Conf. on few body problems in physics, ed. B.K. Jennings, Vancouver (1989) p. C26.
[12] M. Skill, R. Baumann, S. Hoos-Wenzel, G. Keil, N. Kniest, H. Lange, T. Ohly, E. Pfaff, M. Preiss, G. Reiter, G. Clausnitzer, M. Haller and W. Kretschmer, Proc. Int. Conf. on Nuclear Physics, Sao Paulo (1989) p. 7-21.

[13] M. Skill, R. Baumann, G. Keil, N. Kniest, E. Pfaff, M. Preiss, G. Reiter, G. Clausnitzer, M. Haller and W. Kretschmer, Proc. 7th Int. Conf. on polarization phenomena in nuclear physics, Paris (1990) p. 37B.
[14] W. Arnold, H. Berg, H.H. Krause, J. Ulbricht and G. Clausnitzer, Nucl. Instr. Meth. 143 (1977) 441.
[15] W. Arnold, J. Ulbricht, H. Berg, P. Keiner, H.H. Krause, R. Schmidt and G. Clausnitzer, Nucl. Instr. Meth. 143 (1977) 457.
[16] H.H. Krause, R. Stock, W. Arnold, H. Berg, E. Huttel, J. Ulbricht and G. Clausnitzer, Nucl. Instr. Meth. 143 (1977) 467.
[17] A. Hofmann, H. Baumgart, J. Günzel, E. Huttel, N. Kniest, E. Pfaff, G. Reiter, S. Tharraketta and G. Clausnitzer, Proc. 6th Int. Conf. on polarization phenomena in nuclear physics, Osaka (1985), p. 1085.
[18] G. Herrmann, diploma thesis, Giessen (1979).
[19] P. Huber and K.P. Meyer, Proc. Int. Symp. on polarization phenomina of nucleons, Basel (1970).
[20] G.G. Ohlsen and P.W. Keaton Jr., Nucl. Instr. Meth. 109 (1973) 41.
[21] G. Reiter, diploma thesis, Giessen (1982).
[22] J.R. Jenny, Ph. D. thesis, Zürich 1977.
[23] L. Veeser and W. Haeberli, Nucl. Phys. A 115 (1968) 172.
[24] C.H. Johnson, H.B. Willard and J.K. Bair, Phys. Rev. 96 (1954) 985.
[25] H.M. Hofmann, private communication.
[26] M. Herrmann and H.M. Hofmann, private communication.
[27] F. Ajzenberg-Selove, Nucl. Phys. A 490 (1988) 1.